Design optimisation for hybrid metal additive manufacturing for sustainable construction

Baqershahi, Mohammad Hassan; Ayas, Can; Ghafoori, Elyas

Important note
To cite this publication, please use the final published version (if applicable).
Please check the document version above.

Design optimisation for hybrid metal additive manufacturing for sustainable construction

Mohammad Hassan Baqershahi [a,*], Can Ayas [b], Elyas Ghafoori [a]

[a] *Institute for Steel Construction, Faculty of Civil Engineering and Geodetic Science, Leibniz University Hannover, 30167 Hannover, Germany*
[b] *Department of Precision and Microsystems Engineering, Faculty of Mechanical, Maritime and Materials Engineering, Delft University of Technology, 2628CD Delft, the Netherlands*

ABSTRACT

Wire arc additive manufacturing (WAAM) enables the manufacturing of efficient and lightweight structural elements in which material can be utilised wherever needed in an optimised shape, in contrast to standard prismatic profiles used in construction. However, the specific energy consumption (SEC) of WAAM is higher than that of conventional manufacturing (CM) techniques (i.e., hot-rolling) for standard profiles. Therefore, it is an open question whether the material savings through computational design realised via WAAM is environmentally beneficial or not. This systematic study aims to provide a better understanding of the environmental impact of hybrid manufacturing, which is defined as the combination of WAAM and CM rather than using any of them alone. Topology optimisation (TO) is used to design a series of beams with an identical performance (i.e., stiffness) but with a reduced material consumption depending on the hybrid ratio. The environmental impact of the designs has been used to determine when and how hybridisation can become advantageous. The results show that although the optimal proportions of WAAM and CM are dependent on their relative SEC, the hybrid solutions have always been environmentally superior compared to that of WAAM or CM alone for the realistic SEC values, exhibiting up to a 60% reduction in environmental impact compared to that of CM.

1. Introduction

The demand for materials, such as steel, has increased substantially and is expected to continue increasing in the coming years [1,2]. A major consumer of natural resources is the construction sector, which accounts for the largest share of the global carbon footprint [3]. To meet the objectives of the Paris Agreement [4], the challenge is to satisfy the increasing material demand while reducing the overall environmental impact. According to the "Iron and Steel Technology Roadmap" report, at least a 50% reduction in steel industry emissions is necessary by 2050 to achieve net zero carbon emissions [5].

Labour and fabrication costs have been the primary drivers of how structures are built, ranging from uniform rectangular reinforced concrete elements [6] to standard profiles in steel structures. For instance, it has been reported that the average utilisation factor ratio of steel in UK buildings is less than 50% [7]. The construction industry has been slow to incorporate new technologies, such as robotics and 3D printing [8,9], building information modelling [10], cloud computing [11], and virtual reality [12], to enhance productivity and efficiency. Utilising materials

more efficiently can lead to significant emission mitigation because of the existing limitations in the technological shift in steel making [2].

1.1. Optimised lightweight structures and additive manufacturing (AM)

Topology optimisation (TO) is the process of computationally determining the best geometrical layout of a structure for a desired objective without prior assumptions about the shape and connectivity of the members [13] which results in highly efficient yet complex geometries that are prohibitively expensive or impossible to produce using conventional manufacturing (CM) methods. With the development of metal AM technologies, which is envisioned as one of the leading technology for construction transformation [14], new possibilities have been introduced to realise such efficient and optimised structures for real-world applications. Given the inherent synergy between TO and AM, research has also been focused on further development of TO for AM to tailor it for large-scale applications [15], to take into account AM deposition direction [16,17], to consider thermal history during AM for adjusting material properties [18], and to develop new structural design concepts [19–23].

Nomenclature

CM	Conventional Manufacturing	c_0	Maximum allowable compliance
TO	Topology Optimisation	E_e	Young's Moduli of the element e
AM	Additive Manufacturing	E_0	Solid Young's Moduli
BTF	Buy-to-Fly Ratio	E_{min}	Void Young's Moduli
WAAM	Wire and Arc Additive Manufacturing	p	Penalty in SIMP method
LPBF	Laser Powder Bed Fusion	$\tilde{\rho}_e$	Filtered density of the element e
LCA	Life-Cycle Assessment	ω_{ie}	Weighting factor between elements i and e
CNC	Computerised Numerical Control	R	Filter radius
SEC	Specific Energy Consumption	r_{ei}	Centre-to-centre distance between elements i and e
SIMP	Solid Isotropic Material Penalisation	I	Environmental impact
MMA	Method of Moving Asymptotes	r	Relative specific energy consumption
ρ	Density of an element	SEC_{WAAM}	Specific energy consumption of WAAM
W	Weight of the structure	SEC_{CM}	Specific energy consumption of conventional method
K	Global stiffness matrix of the structure	I_i	Environmental impact of a component
u	Vector of nodal displacements	W_i^{CM}	Weight of CM part of beam i
f	Vector of nodal forces	$W_i^{(WAAM)}$	Weight of WAAM part of beam i
c	Compliance of the structure	I_{ref}	Environmental impact of the reference beam
		W_{ref}	Weight of the reference beam

1.2. Metal AM in construction

Metal AM methods have found widespread applications in high-tech and high-end industries, such as the medical, automotive, and aerospace benefiting from on-demand manufacturing, customisation, and shorter lead times [24,25]. For example, the buy-to-fly (BTF) ratios in manufacturing aerospace parts are relatively high [26], and metal AM can significantly reduce production waste compared to conventional subtractive methods. Moreover, material savings due to topology optimisation can substantially reduce fuel consumption and emissions during the operation phase, even if the production of the part has a higher environmental impact than when conventionally manufactured.

AM in the context of the construction industry for significantly larger parts is entirely different. CM processes are mainly forming/extrusion-based, that is, hot rolling and cold forming, which produce meagre waste, unlike subtractive methods. Therefore, the adoption of metal AM in construction is mainly attributed to using less material through topology optimised geometries, which also has the secondary effect of reducing both the gravitational and seismic loads applied on other elements.

Among various metal AM techniques, wire and arc additive manufacturing (WAAM) is suitable for the construction sector because it provides relatively higher deposition rates, no size limitations, and lower cost than other metal AM techniques, e.g. laser powder bed fusion (LPBF) [26,27]. Fig. 1 exhibits two examples of large-scale structures produced with WAAM technology. Various studies have been performed to characterise the mechanical properties of the printed components with WAAM [28–31]. However, the sustainability of WAAM in comparison to CM employed in construction still requires further investigation.

1.3. Environmental impact of metal AM

Generally, any AM technique has various characteristics that contribute to its sustainability [33], such as reduced material use [34] and possible life extension [35]. Numerous studies have compared sustainability of metal AM with CM methods [36–38] with fewer specifically focused on WAAM. Salvi et al. [39] compared sustainability of a wrought part with its counterpart made with WAAM, with an emphasis on machinability of the parts. They found that the total carbon emissions from fabrication and machining of parts made with WAAM exceed the wrought ones [39]. A comparative LCA of WAAM and machining for producing three industrial parts, including a large-scale steel beam,

(a)

(b)

Fig. 1. (a) MX3D Bridge (the first 3D-printed steel bridge) [32], (b) optimised cantilever beam [23] manufactured using WAAM.

revealed that WAAM has a significantly lower cumulative energy demand [40]. Kokare et al. [41] compared WAAM, CNC, and LPBF for the fabrication of simple walls. In this study, although CNC outperformed WAAM in terms of sustainability, the sensitivity analysis revealed that greater geometrical complexities led to lower CNC efficiencies, which made WAAM the most sustainable method. A mass-based LCA comparison of WAAM, CNC, and green sand casting for stainless steel indicated a linear relationship between weight and environmental impact [42]. This observation implies that mass reduction with TO can directly reduce the corresponding impact. A recent study on the LCA of WAAM for producing large-scale structural steel elements also highlighted the potential of WAAM to reduce the environmental impact of structural elements owing to optimisation providing material savings [43].

Despite the material savings offered by WAAM, the method involves

additional steps to those required for the CM of structural sections, as shown in Fig. 2(a) and (b). Therefore, WAAM is more wasteful and energy-consuming than CM to deliver the same amount of material.

Shah et al. [43] estimated that a conventional hot-rolling process requires only 1.04 kg of carbon steel to manufacture 1 kg of carbon steel product, whereas WAAM requires approximately 1.18 kg of carbon steel to manufacture the same product. Bekker and Verlinden [42] reported a slightly larger amount, i.e. 1.3 kg, of raw materials to produce 1 kg of stainless steel using WAAM. Table 1 lists the required materials for the production of 1 kg of stainless steel for each step from raw material extraction to the final product, as reported in [42]. Based on these data, it is possible to estimate the production of 1 kg of stainless steel through hot rolling using CM, as shown in Table 2. Regardless of the exact value, WAAM consistently consumes more material and, subsequently, more energy to deliver 1 kg of material than hot rolling.

1.4. The concept of hybrid manufacturing

Combining AM with CM (i.e. hybrid manufacturing) is generally considered to compensate for the limitations of each manufacturing technique [44]. For example, improved quality and dimensional accuracy can be achieved by combining AM with subtractive techniques [45]. The hybridisation of AM with forming processes can harness the flexibility of the former and the productivity of the latter [45,46]. Several studies have explored the possibility of hybrid manufacturing with forming processes, primarily focusing on process parameters and material characterisation [47,48]. Recent investigations have also explored hybrid manufacturing as a strengthening strategy to improve the stability of I-sections [49,50] and to repair cracked steel members [35], as shown in Fig. 3. The possibility of reducing energy consumption under certain conditions has also been reported [51]. However, the environmental potential for hybrid manufacturing in construction has remained almost disregarded.

This study aims to investigate the hybrid manufacturing of WAAM and CM for fabricating structural elements through an optimisation framework, with the intent of reducing the environmental impact during the design stage. To avoid dependence on specific data for the environmental impact assessment and the SEC of WAAM and CM, a parametric study on SEC was conducted. Therefore, the results can be used and referred to for any given SEC input. The geometrical aspects, including boundary and loading conditions, and percentages of the CM sections were studied. To illustrate how each parameter affects the environmental impact of the designs, two examples were examined: a cantilever and simply supported beam. This study aims to provide a design framework to assess the sustainability of WAAM for large-scale constructions and to fill the gap in engineering design approaches for WAAM as a novel construction technology. Although we can borrow from the established standards for traditional structural design, new requirements and guidelines for using WAAM in construction are required. Therefore, integrating sustainability assessment measures with technical requirements has the potential to be highly important for adopting WAAM successfully and sustainably.

Section 2 explains the methodology for topology optimisation and

Table 1
Material waste/utilisation assumptions for the WAAM process of stainless steel and their contribution to climate change [42].

Process	Waste	Utilisation	Mass	Climate Change (kg CO2 eq/kg stainless steel)	Total
Raw Material Extraction	-	100%	1.298	5.7455	7.460
Continuous Casting	10%	90%	1.298	0.6724	0.873
Hot Rolling	5%	95%	1.169	0.1763	0.206
Wire Drawing	8%	92%	1.110	0.3333	0.370
WAAM process	1.1%	98.9%	1.021	3.6129	3.690
Machining	1%	99%	1.010	0.0057	0.006
Final Product			1		12.605

Table 2
Material waste/utilisation assumptions for the hot-rolling process of stainless steel and their contribution to climate change [42].

Process	Waste	Utilisation	Mass	Climate Change (kg CO2 eq/kg stainless steel)	Total
Raw Material Extraction	-	100%	1.181	5.7455	6.788
Continuous Casting	10%	90%	1.181	0.6724	0.794
Hot Rolling	5%	95%	1.063	0.1763	0.187
Machining	1%	99%	1.010	0.0057	0.006
Final Product			1		7.775

environmental assessments of the structural components. Section 3 provides two 2D case studies of a cantilever beam and simply supported beam using hybrid manufacturing through the proposed optimisation framework to reduce the environmental impact. Section 4 explains the results and discusses their interpretations and practical implications. Finally, Section 5 presents the conclusions of this study.

2. Methodology

2.1. Topology optimisation (TO)

Density-based TO with Solid Isotropic Material Penalisation (SIMP) [13] was used to design the beams. The design domain was discretised into N finite elements, each having a pseudo-density ρ_e with $e = 1, .., N$ ranging between 0 and 1, where $\rho = 0$ represents void and $\rho = 1$ represents solid. In this study, weight minimisation subject to compliance constraint and mechanical equilibrium is considered as follows:

$$\begin{aligned} &\min_{\boldsymbol{\rho}} W \\ s.t.&\mathbf{K}\mathbf{u} = \mathbf{f} \\ &c \leq c_0 \end{aligned} \quad (1)$$

where W is the weight of the structure, $\boldsymbol{\rho}$ is the array of density of each element ρ_e, $\mathbf{K}$ is the global stiffness matrix of the structure, $\mathbf{u}$ is the array
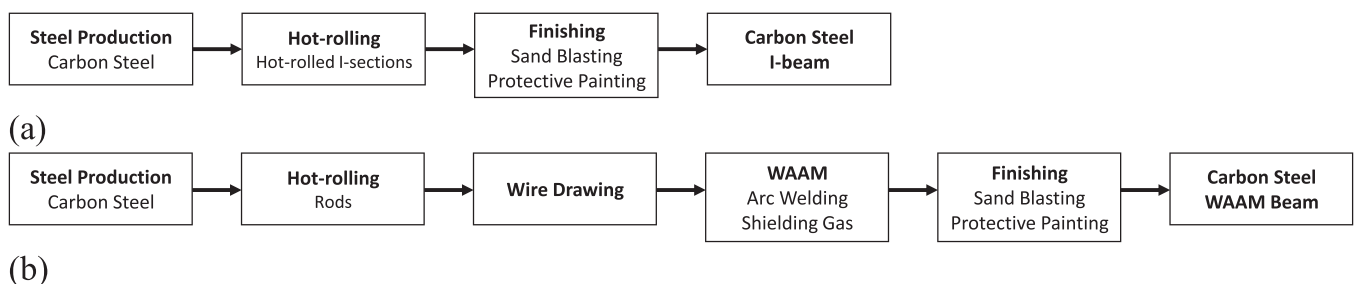

Fig. 2. Schematic of the production steps for a steel beam made using (a) conventional hot-rolling process and (b) WAAM [43].
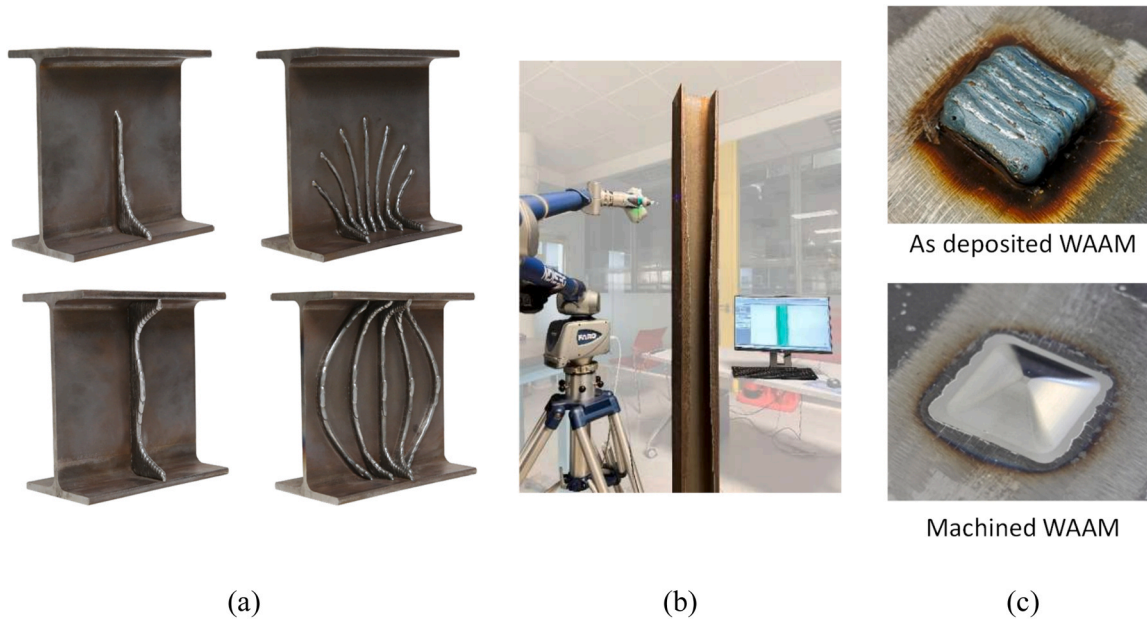
Fig. 3. (a) various WAAM stiffener profiles on IPE profiles [49], (b) WAAM strengthening of I-section column [50], (c) WAAM repair of cracked steel member [35].

of displacements, **f** is the array of applied forces. In addition, c is the compliance of the system, which is computed as $c = \mathbf{f}^{\mathrm{T}}\mathbf{u}$, where c_0 is the maximum allowable compliance of the system. Given the difficulty of solving large-scale integer variable optimisation problems with gradient-based methods, intermediate densities were allowed. Nevertheless, material penalisation was introduced to prevent intermediate densities in the optimised design [52]. The penalisation scheme for E_e, which is the Young's modulus of element e is defined as follows [53]:

$$E_e(\rho) = E_{\min} + \rho^p (E_0 - E_{\min}), \tag{2}$$

where $E_{\min}$ and E_0 are the Young's moduli associated with the void and solid phases, respectively. $E_{\min}$ is an order of magnitude lower than E_0 to prevent the singularity of the stiffness matrix. For densities smaller than one, the intermediate density becomes inefficient for the stiffness by choosing $p > 1$. Typically, $p = 3$ is used for acceptable performance [13].

Some numerical issues are inherent to topology optimisation [52], most notably the chequerboard pattern and mesh dependency. The chequerboard pattern is caused by the artificially high stiffness of the elements when arranged in an orthogonal pattern of void and solid (or $\rho = 0$ and $\rho = 1$ respectively) which resembles a chequerboard pattern [13,52]. The mesh dependency stems from the non-existence of an optimal solution in a continuous domain; therefore, refining the mesh leads to a different but more optimal solution. Both these issues have been overcome using a filtering technique [52]. Density filtering [54] is a type of filtering that considers the neighbourhood of an element to calculate a weighted average of $\widetilde{\rho}_e$ densities.

$$\widetilde{\rho}_e = \frac{1}{\sum\limits_{i \in N} \omega_{ie}} \sum\limits_{i \in N} \omega_{ie} \rho_e, \tag{3}$$

where N is the number of elements within the filter radius R of the element e, and ω_{ie} is the weighting factor, defined as follows:

$$\omega_{ie} = \max(0, R - r_{ei}), \tag{4}$$

where r_{ei} is the centre-to-centre distance between the elements e and i.

The problem was optimised based on an 88-line MATLAB code [53] modified accordingly for this study. The method of moving asymptotes (MMA) [55] was used as the optimisation algorithm.

2.2. Environmental assessment

To estimate the environmental impact I of a component, the total energy consumption from material extraction to production was considered, with a linear relationship with weight, which is in agreement with similar studies [42,43]:

$$I = SEC \cdot W, \tag{5}$$

where SEC is the specific energy consumption, and W is the weight of the component. Determining the exact value of SEC requires a comprehensive LCA, which is beyond the scope of this study. Instead, the SEC of WAAM relative to CM, r, was defined as follows:

$$r = \frac{SEC_{\mathrm{WAAM}}}{SEC_{\mathrm{CM}}}, \tag{6}$$

where SEC_{WAAM} and SEC_{CM} represent the specific energy consumptions of the WAAM and CM processes, respectively. The r value depends on the type of metal and the process parameters of WAAM and CM (e.g. the deposition rate and electricity source [43]).

Based on Table 1 and Table 2, an estimation of r for WAAM and hot rolling of stainless steel can be made. The total equivalent CO2 emission of WAAM and hot-rolling for producing 1 kg of stainless steel is equal to 12.61 and 7.78 kg, respectively, which implies $r \simeq 1.62$. As described in Section ⸎1.3, the SEC is dependent on the assumption of production waste/material utilisation and all the process parameters involved. The relative SEC (r) depends on both the WAAM and CM processes. However, it is expected to be greater than one when comparing WAAM and hot rolling because WAAM involves additional steps (see Section ⸎1.3). For a more comprehensive investigation, a parametric study of r was conducted.

Based on Eq. (5), the environmental impact of the hybrid beam I_i is composed of two terms: the weight of the CM part $W_i^{(\mathrm{CM})}$ multiplied by its corresponding SEC, and the weight of the WAAM profile $W_i^{(\mathrm{AM})}$ multiplied by its SEC, which is $SEC_{\mathrm{WAAM}} = rSEC_{\mathrm{CM}}$.

$$I_i = SEC_{\mathrm{CM}} \cdot W_i^{(\mathrm{CM})} + SEC_{\mathrm{WAAM}} \cdot W_i^{(\mathrm{WAAM})} = SEC_{\mathrm{CM}} \left(W_i^{(\mathrm{CM})} + r \cdot W_i^{(\mathrm{WAAM})} \right) \tag{7}$$

To normalise the environmental impact of the hybrid beam, a reference beam with a standard CM profile and similar structural

performance was considered. The normalised environmental impact of the hybrid beam is expressed as follows:

$$\frac{I_i}{I_{\text{ref}}} = \frac{SEC_{\text{CM}}(W_i^{\text{CM}} + r \cdot W_i^{\text{AM}})}{SEC_{\text{CM}} \cdot W_{\text{ref}}} = \frac{W_i^{\text{CM}} + r \cdot W_i^{\text{AM}}}{W_{\text{ref}}}, \tag{8}$$

If this normalised environmental impact is lower than one, the hybrid beam will have a lower environmental impact than the reference CM beam. For a beam produced entirely by WAAM, the normalised environmental impact is simplified to the following:

$$\frac{I_i}{I_{\text{ref}}} = r \frac{W_i^{\text{WAAM}}}{W_{\text{ref}}}, \tag{9}$$

which implies that, for the environmental impact of the WAAM beam to be similar to that of the CM reference beam, the relative weight reduction or material savings owing to TO should be at least $1/r$. For WAAM to have a lower environmental impact, even greater material savings are required. A case study of the LCA for WAAM and CM also reported a similar relationship between material savings and environmental impacts [43].

3. Results

This section presents two case studies with different loading and boundary conditions, a 2D cantilever beam and a 2D simply supported beam, to apply the optimisation and environmental assessment framework. First, a reference beam with a CM-made profile was defined, with stiffness as the required structural performance for the remaining cases. Second, a beam with no hybridisation was studied to examine the sustainability of WAAM alone. Finally, hybrid beams are presented to offer new designs and extend the possibility of using WAAM to reduce environmental impacts.

3.1. 2D Cantilever beam

A reference cantilever beam made with CM is shown in Fig. 4(a). The beam had an aspect ratio of $L/H = 5$. The design domain for TO was a rectangle of the same length as the reference beam; however, the height of the design domain $H^{'}$ was allowed to exceed that of the reference beam to expand the design space, as shown in Fig. 4(b).

First, as shown in Fig. 5(a), a beam manufactured entirely with WAAM (referred to as the WAAM beam) was assessed. Then, the hybrid beams were investigated, where the beam comprised a part made with CM combined with a WAAM profile, as shown in Fig. 5(b).

3.1.1. WAAM beams

Using TO, a range of alternative optimised beams with no hybridisation were designed to reduce the weight while maintaining structural performance, that is, stiffness. A height increase in the design domain with $H^{'}/H$ ranging from 1.1 to 1.5 was considered. Fig. 6 depicts the optimised designs to be manufactured entirely with WAAM and their weight normalised with respect to the weight of the reference beam as a function of $H^{'}/H$.

To assess the environmental impact, the normalised environmental impact, as per Eq. (9) was used, in which the weight reduction provided by WAAM is offset by the r (relative SEC). For the lightest beam with $H^{'}/H = 1.5$, approximately 65% weight reduction was achieved. Based on Eq.(9), the breakeven point at which the WAAM beam has the same environmental impact as the reference beam is $r = W_{\text{ref}}/W_{\text{AM}} = 1/(1 - 0.65) = 2.86$.

3.1.2. Hybrid beams

To design the hybrid beams, the design domain depicted in Fig. 4(b) was divided into design and nondesign areas. In the design area, the elements can take any value between 0 and 1 (void and solid), whereas the non-design area corresponds to the part of the design made with CM.
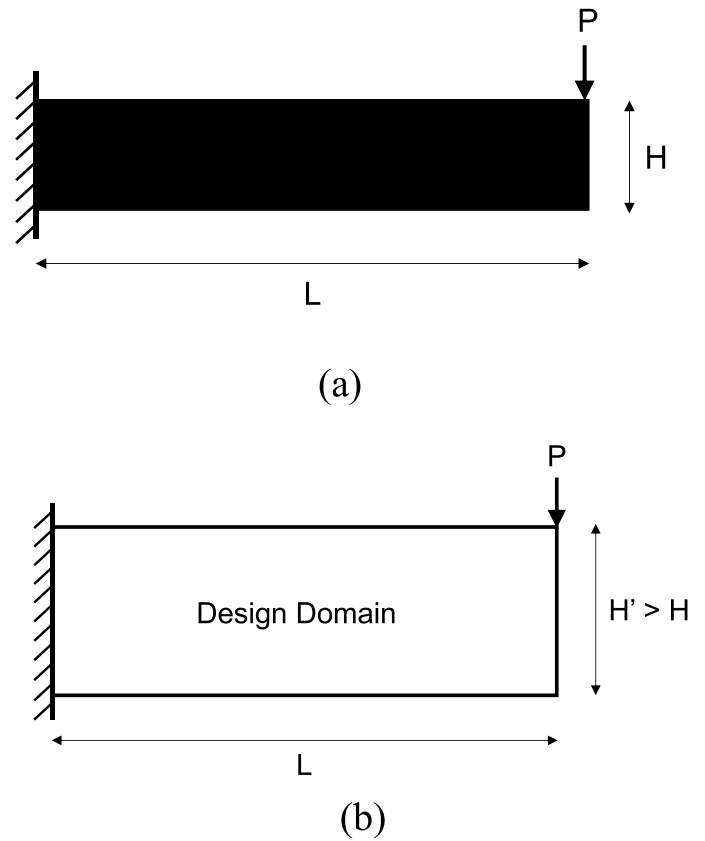

Fig. 4. Geometry, boundary conditions, and loading of the (a) reference CM cantilever beam and (b) design domain for TO.
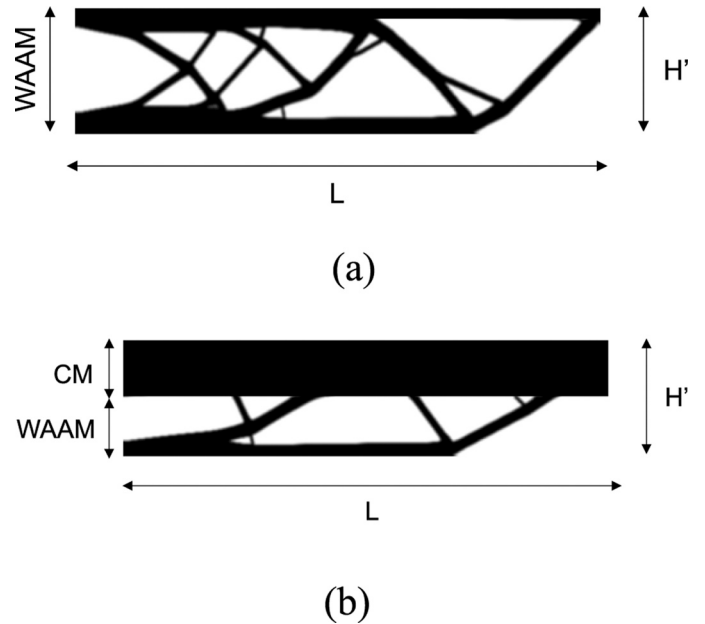

Fig. 5. (a) WAAM beam which is entirely manufactured by WAAM, (b) Hybrid beam which is partly manufactured by WAAM and partly with CM.

In the non-design area, element densities are fixed to $\rho = 1$ during TO. The hybrid ratio is defined as the height of the part made with CM divided by the total height of the beam, $H^{'}$. A range of hybrid ratios was considered for various height increases ($H^{'}/H$) when designing a series of alternative hybrid beams. The optimiser then added an optimal
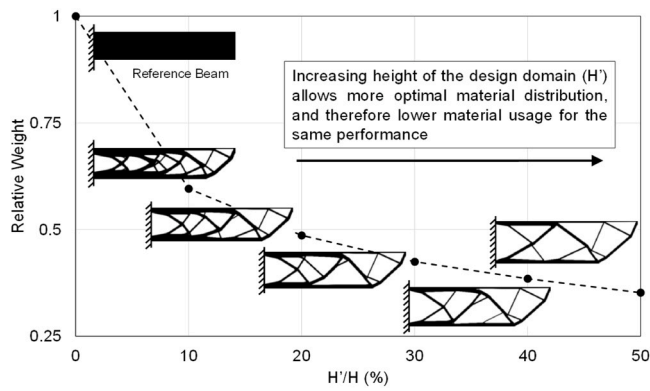
Fig. 6. Normalised weight of the WAAM beams with respect to the weight of the reference beam for different values of H'/H with identical stiffness.

geometrical layout with minimum weight in the design area to achieve the desired stiffness. Table 3 summarises the designs shown in Fig. 7 in terms of H'/H and the hybrid ratio. The weights listed in Table 3 were normalised by dividing the corresponding weight by that of the reference beam.

The normalised environmental impacts of these designs varied depending on the relative SEC of WAAM and CM. The normalised environmental impact of a beam is equal to its normalised weight for the limiting value of $r = 1$, which implies that WAAM and CM have the same SEC. Consequently, the material savings provided by all fully optimised *WAAM beam* designs depicted in Fig. 6 outperformed all the hybrid beams because they were lighter.

However, for more realistic values of $r > 1$ (which imply a higher SEC for WAAM than for CM), the environmental impacts of the designs were no longer directly proportional to the weight. The environmentally optimal design was a trade-off between the lower SEC of the CM and the optimal material distribution provided by WAAM. The normalised environmental impacts of the beams for $r = 1.5$ are shown in Table 4. With a 50% increase in r, the environmental impact of the *WAAM beam* increased by the same amount, i.e., $0.35 \times 1.5 \simeq 0.53$. It still had a 47% lower environmental impact than the reference beam. However, the most sustainable design was the beam with a maximum H'/H of 50% and approximately 10% hybridisation, which has a 53% lower environmental impact than the reference beam.

For greater r values, which assume WAAM to be more environmentally intensive with respect to CM, more of the optimised designs made at least partly with WAAM lost the advantage of being lightweight and sustainable. Fig. 8(a) and (b) show maps of the normalised environmental impacts of the beams for $r = 1.5$ and $r = 3.5$, respectively. The environmental impacts of all designs increased with increasing r.

Fig. 9 provides a more comprehensive view of the environmental assessment of alternative designs for r values ranging from 1.0 to 3.5. Each isocurve corresponds to a series of beams with different H'/H and hybrid ratios but with the same normalised environmental impact.

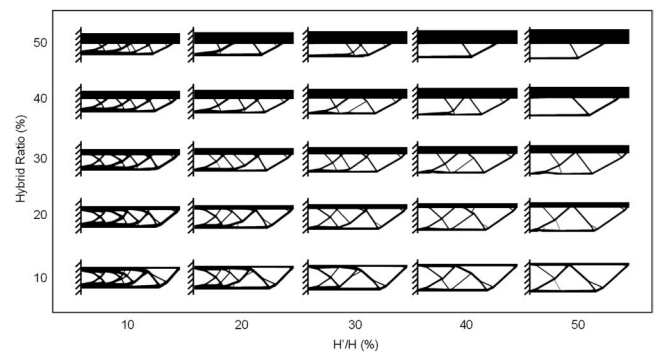The most sustainable design always lay along the maximum "height

Fig. 7. Hybrid cantilever beams with identical stiffness but different H'/H and hybrid ratios.

Table 4
Normalised environmental impacts of the designs for $r = 1.5$ with respect to the reference beam.

Hybrid ratio (%)	H'/H (%)				
	10	20	30	40	50
0	0.89	0.73	0.64	0.58	0.53
10	0.84	0.67	0.58	0.51	0.47
20	0.80	0.66	0.59	0.57	0.55
30	0.79	0.70	0.67	0.67	0.66
40	0.83	0.77	0.76	0.76	0.77
50	0.88	0.84	0.84	0.84	0.85

increase" owing to the more efficient distribution of material further from the neutral axis of the beam, resulting in more material saving. Moreover, with increasing r, the environmentally optimal point shifted along the hybrid ratio axis, indicating that more hybridisation is required to offset the greater impact of WAAM. For the relatively large value of $r = 3.5$, the environmental impact of a WAAM beam was about 20% higher than that of the reference beam. However, a hybrid beam with a lower environmental impact than the reference beam can still be designed, albeit with a limited advantage.

The layout of the isocurves in Fig. 9 also shows that as the height increases, the designs generally become more sensitive to hybridisation for all values of r. For instance, in Fig. 9(b), where $r = 1.5$ and H'/H is approximately 10%, hybridisation between 0–50% yielded nearly identical environmental impacts. However, in the same figure with a H'/H of approximately 50%, each 10% increase in hybridisation changed the normalised environmental impact by about 10%. Furthermore, for r values close to 2, as shown in Fig. 9(a)–(c), increments in the hybrid ratio led to lower sensitivities of the environmental impact with respect to H'/H; for instance, for $r = 1.5$ and a hybrid ratio of approximately 40% (see Fig. 9(b)), beams with an H'/H between 20–50% had nearly the same normalised environmental impact.

Fig. 10 shows the normalised environmental impacts of various designs for a constant H'/H of 50% and different L/H aspect ratios. For

Table 3
Normalised weights of the hybrid cantilever beams with respect to the reference cantilever beam in terms of the part made with CM and with WAAM.

| Hybrid ratio (%)	H'/H (%)														
	10			20			30			40			50		
	WAAM	CM	Total	WAAM	CM	Total	WAAM	CM	Total	WAAM	CM	Total	WAAM	CM	Total
0	0.60	0.00	0.60	0.49	0.00	0.49	0.42	0.00	0.42	0.38	0.00	0.38	0.35	0.00	0.35
10	0.49	0.11	0.60	0.37	0.12	0.49	0.30	0.13	0.43	0.24	0.14	0.38	0.21	0.15	0.36
20	0.39	0.22	0.61	0.28	0.24	0.52	0.22	0.26	0.48	0.19	0.28	0.47	0.17	0.30	0.37
30	0.31	0.33	0.64	0.23	0.36	0.59	0.19	0.39	0.58	0.16	0.42	0.58	0.14	0.45	0.59
40	0.26	0.44	0.70	0.19	0.48	0.67	0.16	0.52	0.68	0.13	0.56	0.69	0.11	0.60	0.71
50	0.22	0.55	0.77	0.16	0.60	0.76	0.13	0.65	0.78	0.09	0.70	0.79	0.07	0.75	0.82
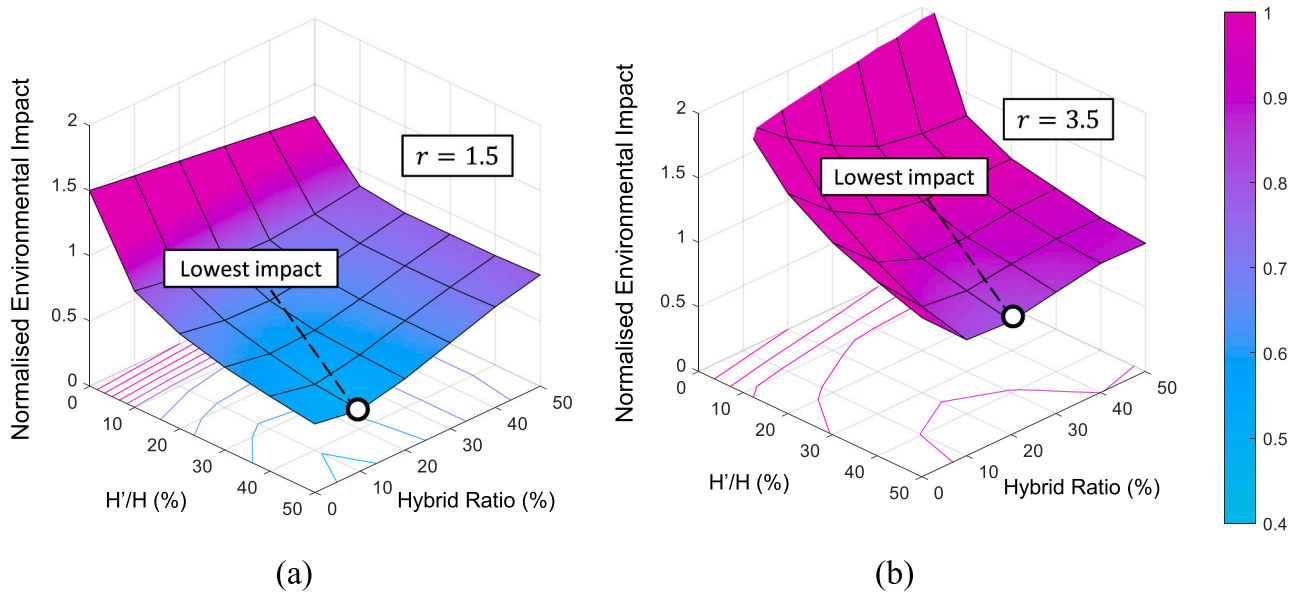
Fig. 8. Normalised environmental impacts of alternative designs to the reference beam for (a) $r = 1.5$ and (b) $= 3.5$. The optimal material distribution of the WAAM is offset by its increasing environmental intensity. Therefore, the design with a larger proportion made with CM becomes more sustainable. In other words, the environmentally optimal design becomes one with a greater hybrid ratio.

various length-to-height ratios, the configurations of the isocurves were similar; for $r > 1$, which implies that WAAM has a higher SEC than CM, there were hybrid beams with a lower environmental impact than the WAAM beam. Moreover, as r increases, the optimal hybrid ratio increased, whereas the gain from optimisation and hybridisation decreased to the point of WAAM is no longer a sustainable option.

The shaded areas correspond to designs that have equal or higher environmental impacts than the reference beam. If the breakeven boundary is defined as the boundary where the environmental impact of the hybrid beams becomes identical to that of the reference beam (iso-curve value 1), then hybridisation bent the breakeven boundary towards a greater r. This indicates a greater possibility of using WAAM, even though its SEC is multiple times that of CM. The effect is more significant at greater length-to-height ratios. As a measure to show the applicability extent of WAAM, the breakeven point can be defined as the point with the highest possible r with the same environmental impact as the reference beam. With that assumption, for $L/H = 3$ the best layout becomes identical to the reference beam at $r \approx 2.9$ (Fig. 10(a)), which is a narrower range than the beam with $L/H = 5$, which happens at $r > 3.5$ which is not visible within the current limits of the figure (Fig. 10(b)). For $L/H = 7$, the breakeven point is even further, which can be traced by looking at isocurves' configuration.

3.2. Simply supported beam

Fig. 11(a) shows a simply supported reference beam with a point load in the middle. This beam was studied to investigate the robustness of the environmental assessment with respect to the load cases. The corresponding design domain with the same length L is shown in Fig. 11 (b). Initially, an aspect ratio of $L/H = 5$ was considered.

3.2.1. WAAM beams

Fig. 12 shows the fully optimised simply supported beam designs and their normalised weights with respect to the reference beam as a function of H'/H. The normalised weight of the lightest beam with a 50% increase in height was approximately 51% that of the reference beam. Therefore, the breakeven point where the WAAM beam and reference beams have equal environmental impacts was at $r = 1/0.51 = 1.96$ (Eq. (9)). This is lower than its cantilever counterpart with a breakeven point of 2.86, resulting from the less significant material savings in this

problem.

3.2.2. Hybrid beams

The introduction of the part made with CM made other design alternatives with various H'/H and hybrid ratios possible, as shown in Fig. 13. The corresponding weights of the hybrid beams are listed in Table 5.

Depending on the r value, the environmental impacts of the beams in Fig. 13 differed. The normalised environmental impacts of the beams based on Eq. (8) are shown in Fig. 14. The trends were similar to those of the cantilever beam (Fig. 9). For the limiting value of $r = 1$, the WAAM beam with the maximum H'/H has the lowest weight and environmental impact. However, the hybrid beams became more sustainable for a greater r. At approximately $r = 2.5$, all designs in Fig. 13 became equal to or worse than the reference beam in terms of the environmental impact. For the cantilever beam, this occurred at approximately $r > 3.5$.

Fig. 15 shows the normalised environmental impacts of the hybrid designs for a constant H'/H of 50% and different length-to-height aspect ratios. Similar to the previous example, for $r > 1$, hybridisation can always lead to a lower environmental impact compared with a beam manufactured entirely with WAAM. For a greater r, a greater hybrid ratio was required to compensate for the higher SEC of WAAM in all cases. The r value at the breakeven point is dictated by the aspect ratio of the beam. For $L/H = 3, 5, 7, 9, 11, 13$ the breakeven points were $r = 1.8$, $2.5, 3.1, 3.8, 4.1$ and 4.5 respectively. This indicates that for greater length-to-height ratios, the possibility of using WAAM to reduce the environmental impact is possible for a broader range of r. This is reflected by the shrinking of the shaded area which corresponds to the designs with a higher environmental impact than the reference beam.

A comparison between the results of simply supported beams in Fig. 15(a-c) with those of cantilever beams in Fig. 10 shows that, for a given length-to-height aspect ratio, the use of WAAM for enhanced sustainability is beneficial for relatively greater r values of cantilever beams. However, the breakeven point of simply supported beams can also exceed $r > 3.5$, when more practical length-to-height ratios are considered, as shown in Fig. 15 (d-e).
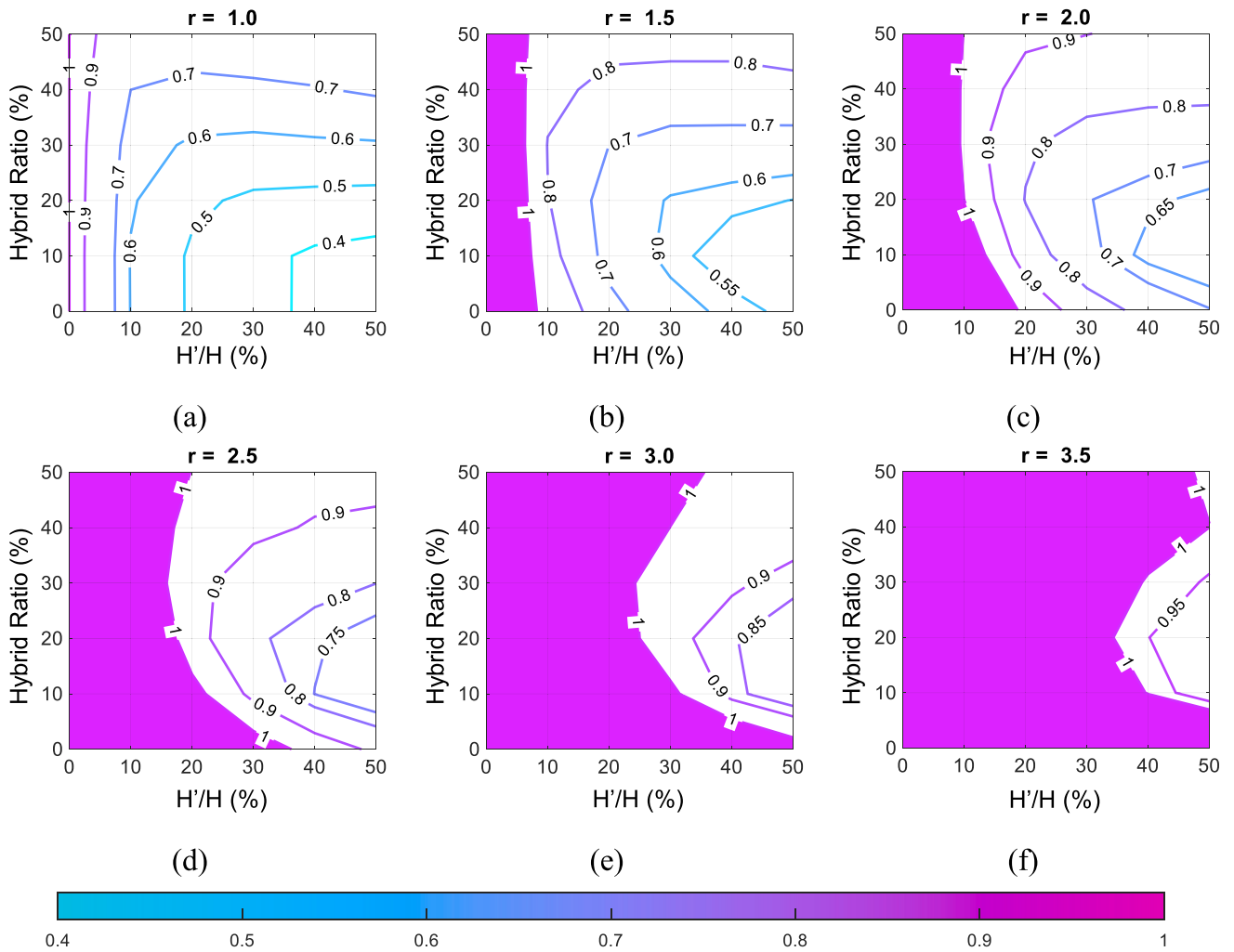
Fig. 9. Normalised environmental impacts of various designs with respect to the reference beam for a range between (a) $r = 1$ to (f) $r = 3.5$. As r increases, more of the design alternatives lose their environmental advantage over the reference beam, as shown by the shaded area. However, even for r as high as 3.5, it is possible to design hybrid beams with lower environmental impact than the reference beam. Each isocurve corresponds to a series of designs with the same environmental impact yet different shapes and weights.
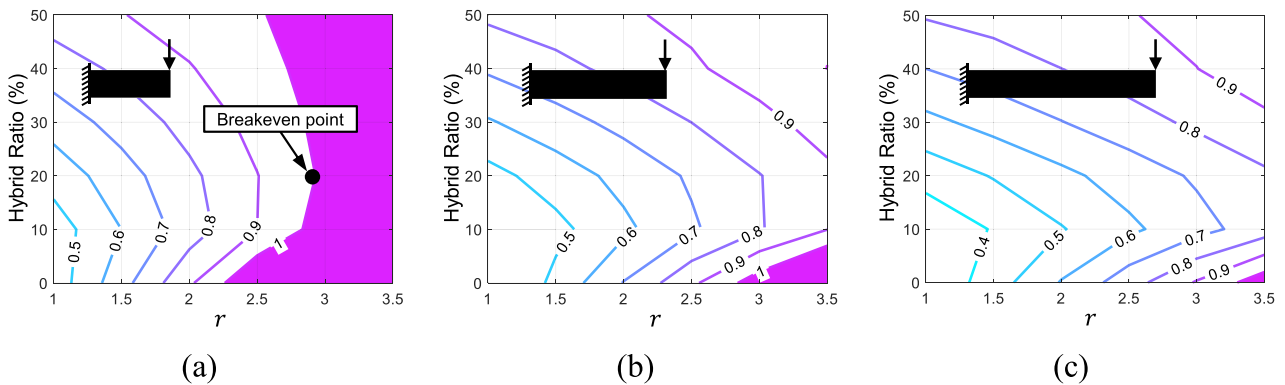

Fig. 10. Normalised environmental impacts of designs for a constant H'/H of 50% with respect to the hybrid ratio and r; (a) $L/H = 3$, (b) $L/H = 5$, (c) $L/H = 7$. The shaded area shows the region beyond which the designs have higher environmental impacts than the reference beam. In all cases, hybridisation bends this area towards a greater r, allowing sustainable designs for even greater r values compared to the WAAM beam. As r increases, a greater ratio of hybridisation leads to a lower environmental impact.
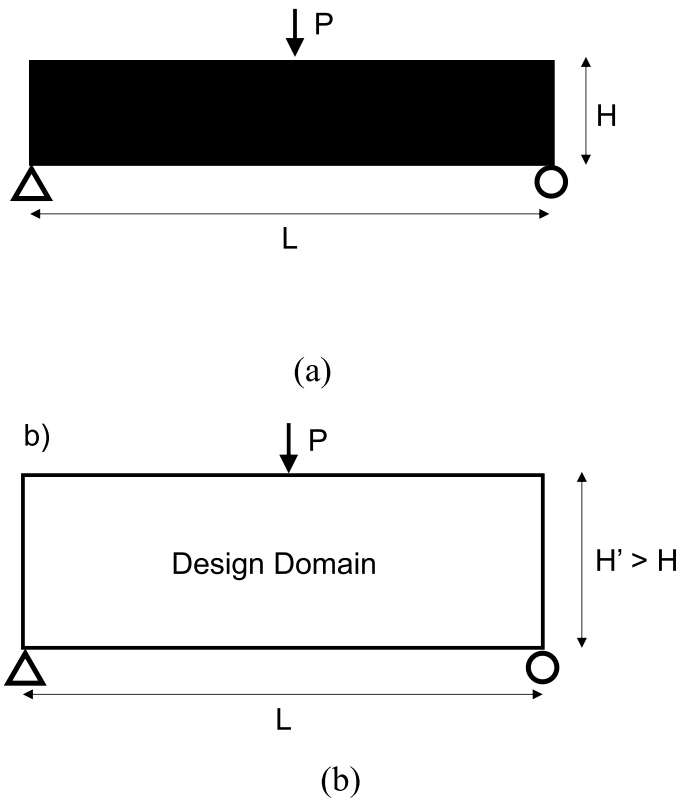
(a)

(b)

Fig. 11. Geometry, boundary conditions, and loading of the (a) reference simply supported beam with CM. (b) Design domain for TO.
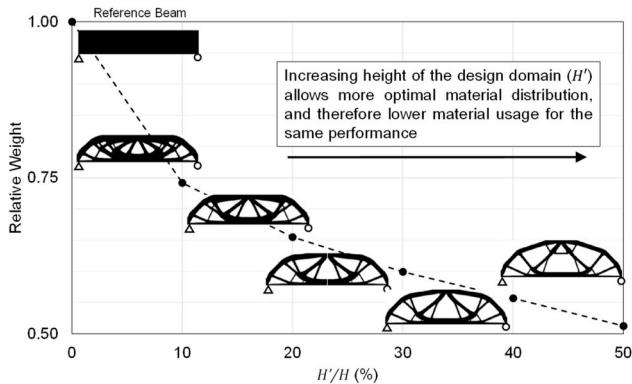

Fig. 12. Normalised weight of the optimised simply supported beams with respect to the weight of the reference beam for different values of H'/H with identical stiffness.

4. Discussion

4.1. Hybrid manufacturing for construction

A parametric study of the relative SEC of WAAM to CM (r) provided a comprehensive overview of when and how hybridisation can be utilised towards achieving sustainability in structural design. The value of r was shown to be a key factor in determining the environmental impact of the design. For $r \approx 1$, the hybrid beam had no environmental superiority. However, for r values greater than one, hybridisation can be an effective strategy for harnessing the advantages of WAAM, offsetting its higher SEC and thereby offering more sustainable design alternatives. A hybrid beam weighs less than a beam made with CM, and yet it is heavier than a fully optimised beam made solely with WAAM. However, it has a lower
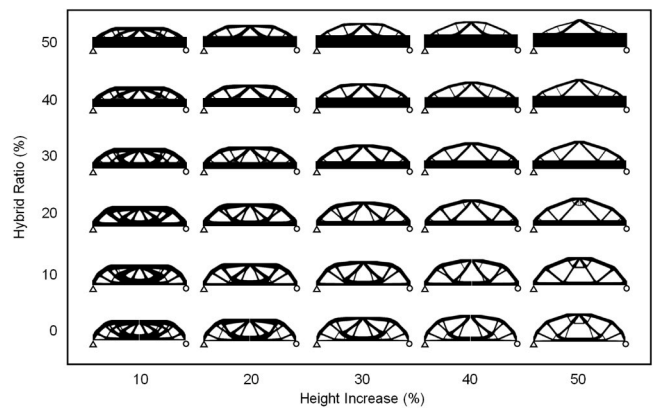

Fig. 13. Hybrid simply supported beams with identical stiffness but different H'/H and hybrid ratios.

environmental impact than both of them, which could be up to 60%. Rethinking and redesigning structural elements using hybrid manufacturing could be particularly important for the construction industry, which consumes large amounts of steel and produces significant emissions.

The examples demonstrated that the viability of WAAM also depends on geometrical aspects, boundary conditions, and loadings of the problem, as well as the choice of the part made with CM. This can be a reflection of the amount of material savings provided by optimisation in comparison with the sections made with CM. For greater aspect ratios, TO provides greater material savings, justifying the wider range of r values for WAAM. For a given L/H ratio, more material savings were possible for the cantilever beam than for the simply supported beam, which resulted in a broader range of applicability of WAAM.

It can also be observed from the results (Fig. 7 and Fig. 13) that greater beam heights led to the optimal designs becoming more truss-like. Although it might seem possible to construct a truss using parts made with CM to achieve a lower environmental impact, the geometrical complexity of the optimal designs results in nodes that are difficult or impossible to build using CM. Furthermore, the size of the members might not match the standard size of the sections, nor might they have a uniform cross-section. Nevertheless, there is room to leverage CM and WAAM more optimally. Instead of a fixed position and length for sections made with CM, the TO algorithm can be modified to determine the best configuration for sections made with CM combined with the added WAAM profiles. In other words, a more optimal combination of WAAM and CM parts is yet to be found to utilise WAAM more effectively towards achieving more sustainability.

4.2. Determination of relative SEC r

The relative SEC (r) depends on several factors, including the type of metal, process parameters, and CM technology. The contributions of these factors to the SEC should be calculated as accurately as possible. For instance, one study compared WAAM and machining to produce a beam made of carbon steel, showing that WAAM resulted in lower CO_2 emissions [40]. However, machining is not a conventional technique for structural elements. Based their report, the r value for WAAM and machining was approximately 0.58, highlighting the lower SEC of WAAM to deliver the same weight as a subtractive method, such as machining with a high BTF ratio. In such cases, WAAM alone is superior to CM, and hybridisation is irrelevant.

4.3. Outlook

This study proposes a design optimisation framework that considers the sustainability of metallic structures. Hybridisation has been

Table 5

Normalised weights of the hybrid simply supported beams with respect to the reference simply supported beam in terms of the part made with CM and with WAAM.

| Hybrid ratio (%)	H'/H (%)														
	10			20			30			40			50		
	WAAM	CM	Total	WAAM	CM	Total	WAAM	CM	Total	WAAM	CM	Total	WAAM	CM	Total
0	0.74	0.00	0.74	0.66	0.00	0.66	0.60	0.00	0.60	0.56	0.00	0.56	0.51	0.00	0.51
10	0.63	0.11	0.74	0.54	0.12	0.66	0.47	0.13	0.60	0.42	0.14	0.56	0.37	0.15	0.52
20	0.53	0.22	0.75	0.43	0.24	0.67	0.37	0.26	0.63	0.31	0.28	0.59	0.28	0.30	0.58
30	0.44	0.33	0.77	0.35	0.36	0.71	0.30	0.39	0.69	0.26	0.42	0.68	0.23	0.45	0.68
40	0.36	0.44	0.80	0.29	0.48	0.77	0.25	0.52	0.77	0.21	0.56	0.77	0.18	0.60	0.78
50	0.29	0.55	0.84	0.23	0.60	0.83	0.19	0.65	0.84	0.16	0.70	0.86	0.13	0.75	0.88

(a)   (b)   (c)
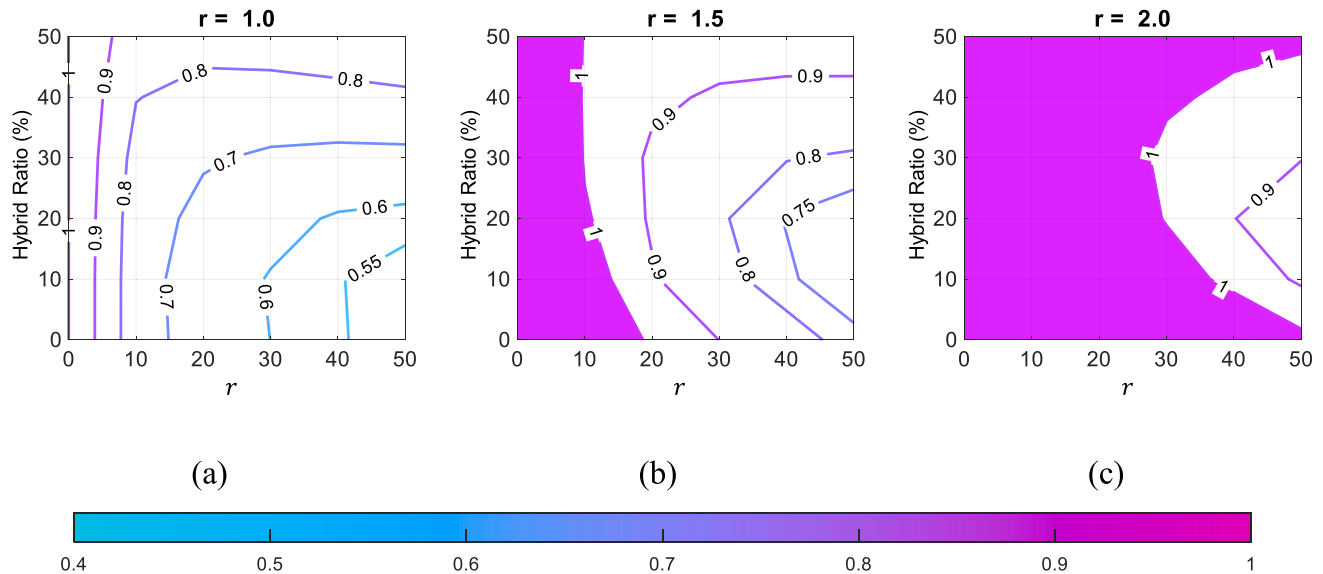
Fig. 14. Normalised environmental impact of various designs with respect to the reference beam for a range between (a) $r = 1$ to (c) $r = 2.0$. As r increases, more of the design alternatives lose their environmental advantage over the reference beam, as shown here by the shaded area. For r of up to approximately 2, it is still possible to use WAAM sustainably. Each isocurve corresponds to a series of designs with the same environmental impact yet different shapes and weights.

suggested as a viable route for reducing the environmental impact of structural components. One of the advantages of the proposed framework is that it can be used to assess different design layouts for other material types and AM techniques. Nevertheless, the examples in this study were mainly selected regarding steel structural elements and WAAM for construction.

To highlight the proposed concept and explain the design framework for sustainability with hybridisation, 2D cantilever and simply supported beams were considered. Based on this, future works could consider 3D examples and other constraints, such as the buckling of members, stress concentrations, manufacturability, and cost. The design space can also be expanded by consideration of multi materials, for either standard profiles or WAAM deposition, providing a greater range of opportunities for innovative structural design solutions. Furthermore, many sub-optimal solutions exist in the design space with the same environmental impact (isocurves in Fig. 9 and Fig. 14) but different characteristics, such as weight and manufacturability, enabling further optimisation based on them.

5. Conclusion

This study proposes a hybrid manufacturing method to reduce the environmental impact of the large-scale usage of metal AM in construction. A set of alternative solutions with various height increases and hybrid ratios was studied, utilising TO for designing optimised beams with the same stiffness as a reference beam made with CM. A linear relationship between the environmental impact and weight was considered, and a comparative environmental assessment was conducted between beams made via CM and those made via hybrid manufacturing. This comparison was performed with respect to the relative SEC of WAAM to CM, r. The following conclusions were drawn:

- For WAAM to be sustainable when used alone to produce an optimised beam, material savings should be at least greater than $1/r$ of the reference beam made via CM.
- There is a direct correlation between the weight reduction and environmental impact for the limiting value of $r = 1$, which translates to a similar SEC for WAAM and CM. This relationship is invalid for more realistic values of r that are typically greater than one. In such cases, the lower environmental impact corresponds not to a lower weight but to a trade-off between the lower SEC of CM and the optimal material distribution of WAAM. A hybrid beam that is heavier than a fully optimised beam but lighter than a beam made with CM and has the lowest environmental impact than both.
- Hybridisation shifts the breakeven point (the point at which producing beams using WAAM and beams using CM have similar environmental impacts) towards greater values of r compared to the shift produced using WAAM alone. This shift increases the viability of WAAM.
- The optimal hybrid ratio depends on the relative SEC of WAAM and CM. For a higher relative SEC, the lowest environmental impact was achieved at a greater hybrid ratio.
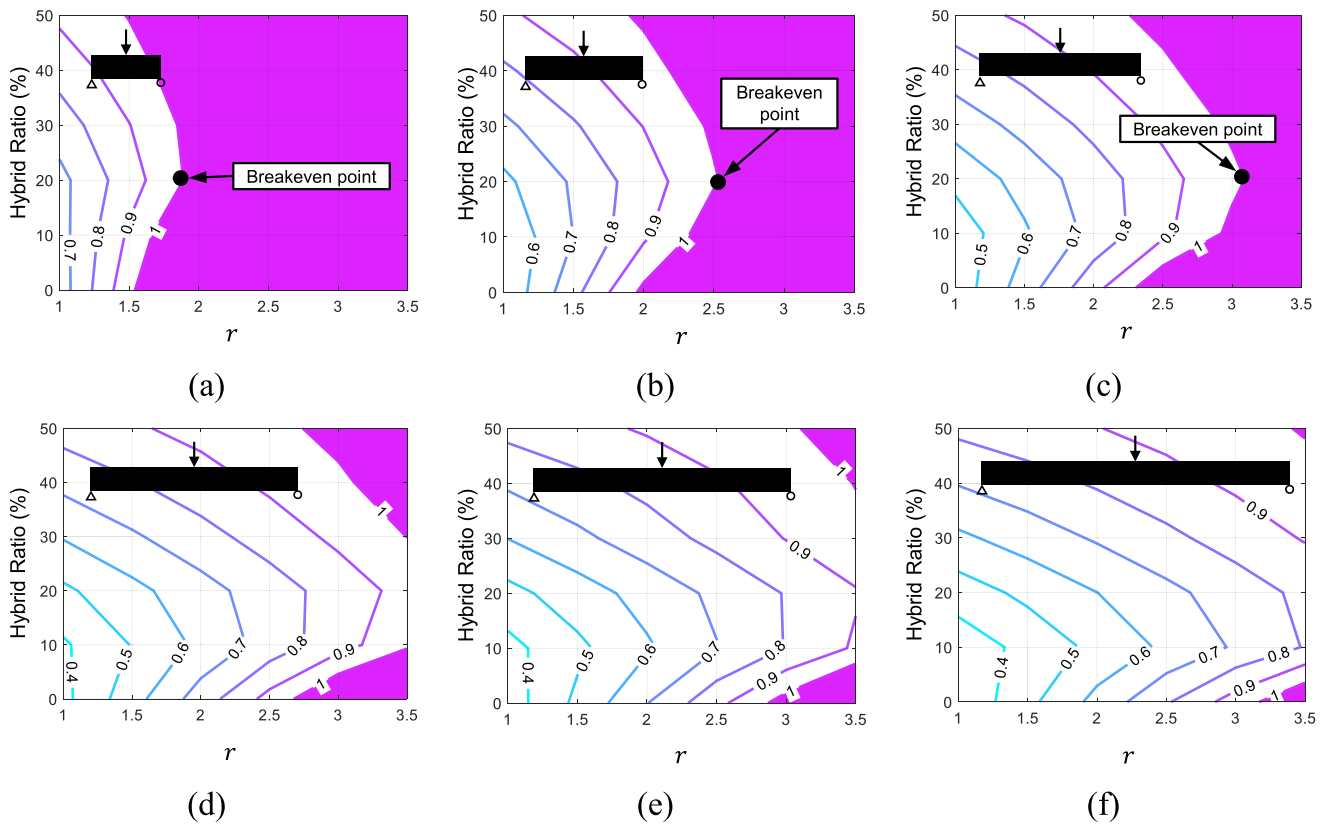
Fig. 15. Normalised environmental impact of designs for a constant $\acute{H}/H$ of 50% with respect to hybrid ratio and *r* value; (a) $L/H = 3$, (b) $L/H = 5$, (c) $L/H = 7$, (d) $L/H = 9$, (e) $L/H = 11$, (f) $L/H = 13$. The shaded area shows the region beyond which designs have a higher environmental impact than the reference beam. In all cases, hybridisation is bending this area towards a greater *r*, allowing to have sustainable design for even greater *r* values compared to the WAAM beam. As *r* increases, the greater ratio of hybridisation leads to a lower environmental impact.

- For greater length-to-height ratios, more material savings are possible. Therefore, WAAM can be used for a greater range of *r* values.
- For a given length-to-height ratio, the cantilever beams had larger breakeven points than the simply supported beams. This shows that while the trends are similar, the extent of viability of WAAM is problem-dependent.

Although technological advances that reduce *r* can broaden the sustainable design space provided by WAAM, this study concludes that, from an environmental perspective, using WAAM alone is unsuitable for large-scale constructions. This is because *r* is generally greater than one in the scope of construction and is expected to remain so owing to the WAAM method taking more steps than the CM process. However, using a hybrid of CM and WAAM could be more promising. This study suggests a framework that can be used for the systematic study of different layouts to design for sustainability.

CRediT authorship contribution statement

Mohammad Hassan Baqershahi: Conceptualization, Methodology, Software, Visualization, Validation, Writing – original draft, Writing – review & editing. **Can Ayas:** Conceptualization, Methodology, Validation, Supervision, Writing – review & editing. **Elyas Ghafoori:** Conceptualization, Methodology, Validation, Supervision, Project administration, Funding acquisition, Writing – review & editing.

Declaration of Competing Interest

The authors declare that they have no known competing financial interests or personal relationships that could have appeared to influence the work reported in this paper.

Data Availability

Data will be made available on request.

References

[1] European Commission; Directorate-General for Climate Action (2019) *Going climate-neutral by 2050 – A strategic long-term vision for a prosperous, modern, competitive and climate-neutral EU economy*. Publications Office.

[2] IEA (2019) *Material efficiency in clean energy transitions*. ⟨https://www.iea.org/reports/material-efficiency-in-clean-energy-transitions⟩.

[3] United Nations Environment Programme 2022 Global Status Report for Buildings and Construction: Towards a Zero-emission, Efficient and Resilient Buildings and Construction Sector. 978–92-807–3984-8. ⟨https://wedocs.unep.org/handle/20.500.11822/41133⟩.

[4] United Nations Environment Programme (2015) Paris Agreement.

[5] IEA Iron and Steel Technology Roadmap [Zugriff am: ⟨https://www.iea.org/reports/iron-and-steel-technology-roadmap⟩].

[6] Kloft H, Empelmann M, Hack N, Herrmann E, Lowke D. Reinforcement strategies for 3D-concrete-printing. Civ Eng Des 2020;2(Nr. 4):131–9. https://doi.org/10.1002/cend.202000022.

[7] Moynihan MC, Allwood JM. Utilization of structural steel in buildings in: proceedings. mathematical, physical, and engineering sciences 2014;470(Nr. 2168):20140170. https://doi.org/10.1098/rspa.2014.0170.

[8] Davila Delgado, J.M.; Oyedele, L.; Ajayi, A.; Akanbi, L.; Akinade, O.; Bilal, M.; Owolabi, H. (2019) Robotics and automated systems in construction: Understanding industry-specific challenges for adoption in: 2352–7102 26, S. 100868. ⟨https://doi.org/10.1016/j.jobe.2019.100868⟩.

[9] El-Sayegh S, Romdhane L, Manjikian S. A critical review of 3D printing in construction: benefits, challenges, and risks (S) : Arch Civ Mech Eng 2020;20(H. 2):1–25. https://doi.org/10.1007/s43452-020-00038-w.

[10] Haghir S, Haghnazar R, Saghafi Moghaddam S, Keramat D, Matini MR, Taghizade K. BIM based decision-support tool for automating design to fabrication process of freeform lattice space structure in. Int J Space Struct 2021;36(Nr. 3):164–79. https://doi.org/10.1177/09560599211033867.

[11] Bello, S.A.; Oyedele, L.O.; Akinade, O.O.; Bilal, M.; Davila Delgado, J.M.; Akanbi, L. A.; Ajayi, A.O.; Owolabi, H.A. (2021) Cloud computing in construction industry: Use cases, benefits and challenges in: 0926–5805 122, S. 103441. ⟨https://doi.org/10.1autcon.2020.103441⟩.

[12] Fernandes KJ, Raja V, White A, Tsinopoulos C-D. Adoption of virtual reality within construction processes: a factor analysis approach. Technovation 2006;26(H. 1, S):111–20. https://doi.org/10.1016/j.technovation.2004.07.013.

[13] Bendsøe MP. Topology Optimization – Theory, Methods, and Applications. 2. Aufl. Berlin, Heidelberg: Springer Berlin Heidelberg; 2004.

[14] European Commission; Executive Agency for Small and Medium-sized Enterprises. Supporting digitalisation of the construction sector and SMEs – Including building information modelling. Publications Office of the European Union; 2019.

[15] Fernández E, Ayas C, Langelaar M, Duysinx P. Topology optimisation for large-scale additive manufacturing: generating designs tailored to the deposition nozzle size. Virtual Phys Prototyp 2021;16(H. 2, S):196–220. https://doi.org/10.1080/17452759.2021.1914893.

[16] Mishra V, Ayas C, Langelaar M, van Keulen F. Simultaneous topology and deposition direction optimization for Wire and Arc Additive Manufacturing in. Manuf Lett 2022;31(S):45–51. https://doi.org/10.1016/j.mfglet.2021.05.011.

[17] Bruggi M, Laghi V, Trombetti T. Simultaneous design of the topology and the build orientation of Wire-and-Arc Additively Manufactured structural elements. : Comput Struct 2021;242(S):106370. https://doi.org/10.1016/j.compstruc.2020.106370.

[18] Mishra V, Ayas C, Langelaar M. Design for material properties of additively manufactured metals using topology optimization. : Mater Des 2023;235(S):112388. https://doi.org/10.1016/j.matdes.2023.112388.

[19] Laghi V, Palermo M, Bruggi M, Gasparini G, Trombetti T. Blended structural optimization for wire-and-arc additively manufactured beams. : Prog Addit Manuf 2023;8, H(3, S):381–92. https://doi.org/10.1007/s40964-022-00335-1.

[20] Kanyilmaz A, Berto F, Paoletti I, Caringal RJ, Mora S. Nature-inspired optimization of tubular joints for metal 3D printing. : Struct Multidiscip Optim 2021;63(H. 2, S):767–87. https://doi.org/10.1007/s00158-020-02729-7.

[21] Wang H, Du W, Zhao Y, Wang Y, Hao R, Yang M. Joints for treelike column structures based on generative design and additive manufacturing. : J Constr Steel Res 2021;184(S):106794. https://doi.org/10.1016/j.jcsr.2021.106794.

[22] Reimann J, Henckell P, Ali Y, Hammer S, Rauch A, Hildebrand J, Bergmann JP. Production of topology-optimised structural nodes using arc-based, additive manufacturing with GMAW welding process. : J Civ Eng Constr 2021;10(Nr. 2):101–7. https://doi.org/10.32732/jcec.2021.10.2.101.

[23] Ye J, Kyvelou P, Gilardi F, Lu H, Gilbert M, Gardner L. An end-to-end framework for the additive manufacture of optimized tubular structures. IEEE Access 2021;9(S):165476–89. https://doi.org/10.1109/access.2021.3132797.

[24] Kanyilmaz A, Demir AG, Chierici M, Berto F, Gardner L, Kandukuri SY, Kassabian P, Kinoshita T, Laurenti A, Paoletti I, Du Plessis A, Razavi N. Role of metal 3D printing to increase quality and resource-efficiency in the construction sector. : Addit Manuf 2022;50(S):102541. https://doi.org/10.1016/j.addma.2021.102541.

[25] Ding D, Pan Z, Cuiuri D, Li H. Wire-feed additive manufacturing of metal components: technologies, developments and future interests. : Int J Adv Manuf Technol 2015;81(1-4, S):465–81. https://doi.org/10.1007/s00170-015-7077-3.

[26] Williams SW, Martina F, Addison AC, Ding J, Pardal G, Colegrove P. Wire + arc additive manufacturing. : Mater Sci Technol 2016;32(H. 7, S):641–7. https://doi.org/10.1179/1743284715Y.0000000073.

[27] Buchanan C, Gardner L. Metal 3D printing in construction: a review of methods, research, applications, opportunities and challenges. : Eng Struct 2019;180(S):332–48. https://doi.org/10.1016/j.engstruct.2018.11.045.

[28] Laghi V, Palermo M, Gasparini G, Veljkovic M, Trombetti T. Assessment of design mechanical parameters and partial safety factors for Wire-and-Arc Additive Manufactured stainless steel in. Eng Struct 2020;225(S):111314. https://doi.org/10.1016/j.engstruct.2020.111314.

[29] Laghi V, Palermo M, Tonelli L, Gasparini G, Ceschini L, Trombetti T. Tensile properties and microstructural features of 304L austenitic stainless steel produced by wire-and-arc additive manufacturing. : Int J Adv Manuf Technol 2020;106(9-10, S):3693–705. https://doi.org/10.1007/s00170-019-04868-8.

[30] Huang C, Zheng Y, Chen T, Ghafoori E, Gardner L. Fatigue crack growth behaviour of wire arc additively manufactured steels. : Int J Fatigue 2023;173(S):107705. https://doi.org/10.1016/j.ijfatigue.2023.107705.

[31] Huang C, Li L, Pichler N, Ghafoori E, Susmel L, Gardner L. Fatigue testing and analysis of steel plates manufactured by wire-arc directed energy deposition. : Addit Manuf 2023;73(S):103696. https://doi.org/10.1016/j.addma.2023.103696.

[32] [Cannot display reference "Adriaan de Groot – MX3D Bridge": Template "Bibliography - Unknown - (Default template)" is not defined.].

[33] Hegab H, Khanna N, Monib N, Salem A. Design for sustainable additive manufacturing: a review. : Sustain Mater Technol 2023;35:e00576. https://doi.org/10.1016/j.susmat.2023.e00576.

[34] Ford, S.; Despeisse, M. (2016) Additive manufacturing and sustainability: an exploratory study of the advantages and challenges in: 0959–6526 137, S. 1573–1587. https://doi.org/10.1016/j.jclepro.2016.04.150.

[35] Ghafoori E, Dahaghin H, Diao C, Pichler N, Li L, Mohri M, Ding J, Ganguly S, Williams S. Fatigue strengthening of damaged steel members using wire arc additive manufacturing. : Eng Struct 2023;284(S):115911. https://doi.org/10.1016/j.engstruct.2023.115911.

[36] Liu Z, Jiang Q, Cong W, Li T, Zhang H-C. Comparative study for environmental performances of traditional manufacturing and directed energy deposition processes. : Int J Environ Sci Technol 2018;15(H. 11, S):2273–82. https://doi.org/10.1007/s13762-017-1622-6.

[37] Mecheter A, Tarlochan F, Kucukvar M. A review of conventional versus additive manufacturing for metals: life-cycle environmental and economic analysis. : Sustain 2023;15(Nr. 16):12299. https://doi.org/10.3390/su151612299.

[38] DeBoer B, Nguyen N, Diba F, Hosseini A. Additive, subtractive, and formative manufacturing of metal components: a life cycle assessment comparison. : Int J Adv Manuf Technol 2021;115(1-2, S):413–32. https://doi.org/10.1007/s00170-021-07173-5.

[39] Salvi H, Vesuwala H, Raval P, Badheka V, Khanna N. *Sustainability analysis of additive + subtractive manufacturing processes for Inconel 625* in. Sustain Mater Technol 2023;35:e00580. https://doi.org/10.1016/j.susmat.2023.e00580.

[40] Priarone PC, Pagone E, Martina F, Catalano AR, Settineri L. Multi-criteria environmental and economic impact assessment of wire arc additive manufacturing in. CIRP Ann 2020;69(H. 1, S):37–40. https://doi.org/10.1016/j.cirp.2020.04.010.

[41] Kokare S, Oliveira JP, Santos TG, Godina R. Environmental and economic assessment of a steel wall fabricated by wire-based directed energy deposition. : Addit Manuf 2023;61(S):103316. https://doi.org/10.1016/j.addma.2022.103316.

[42] Bekker AC, Verlinden JC. Life cycle assessment of wire + arc additive manufacturing compared to green sand casting and CNC milling in stainless steel in. J Clean Prod 2018;177(S):438–47. https://doi.org/10.1016/j.jclepro.2017.12.148.

[43] Shah IH, Hadjipantelis N, Walter L, Myers RJ, Gardner L. Environmental life cycle assessment of wire arc additively manufactured steel structural components. : J Clean Prod 2023;389(S):136071. https://doi.org/10.1016/j.jclepro.2023.136071.

[44] Lorenz, K.A.; Jones, J.B.; Wimpenny, D.I.; Jackson, M.R. (2015) *A Review of Hybrid Manufacturing.* University of Texas at Austin.

[45] Pragana, J.; Sampaio, R.; Bragança, I.; Silva, C.; Martins, P. (2021) Hybrid metal additive manufacturing: A state–of–the-art review in: 2666–9129 2, S. 100032. ⟨https://doi.org/10.1016/j.aime.2021.100032⟩.

[46] Merklein, M.; Junker, D.; Schaub, A.; Neubauer, F. (2016) Hybrid Additive Manufacturing Technologies – An Analysis Regarding Potentials and Applications in: 1875–3892 83, S. 549–559. ⟨https://doi.org/10.1016/j.phpro.2016.08.057⟩.

[47] Ambrogio G, Gagliardi F, Muzzupappa M, Filice L. Additive-incremental forming hybrid manufacturing technique to improve customised part performance in. J Manuf Process 2019;37(S):386–91. https://doi.org/10.1016/j.jmapro.2018.12.008.

[48] Bambach, M. (2016) Recent trends in metal forming: From process simulation and microstructure control in classical forming processes to hybrid combinations between forming and additive manufacturing in: 1895–7595.

[49] Kloft H, Schmitz LP, Müller C, Laghi V, Babovic N, Baghdadi A. Experimental application of robotic wire-and-arc additive manufacturing technique for strengthening the I-beam profiles in. Buildings 2023;13(Nr. 2):366. https://doi.org/10.3390/buildings13020366.

[50] Gardner, L.; Li, J.; Meng, X.; Huang, C.; Kyvelou, P. (2023) *Buckling tests on I-section steel columns strengthened by additive manufacturing* in: ce/papers 6, 3–4, pp. 720–725. ⟨https://doi.org/10.1002/cepa.2462⟩.

[51] Bambach MD, Bambach M, Sviridov A, Weiss S. New process chains involving additive manufacturing and metal forming – a chance for saving energy? : Procedia Eng 2017;207(S):1176–81. https://doi.org/10.1016/j.proeng.2017.10.1049.

[52] Sigmund O, Petersson J. Numerical instabilities in topology optimization: a survey on procedures dealing with checkerboards, mesh-dependencies and local minima in. Struct Multidiscip Optim 1998;16(H. 1, S):68–75. https://doi.org/10.1007/BF01214002.

[53] Andreassen E, Clausen A, Schevenels M, Lazarov BS, Sigmund O. Efficient topology optimization in MATLAB using 88 lines of code. : Struct Multidiscip Optim 2011;43(H. 1, S):1–16. https://doi.org/10.1007/s00158-010-0594-7.

[54] Bourdin B. Filters in topology optimization. : Int J Numer Methods Eng 2001;50(Nr. 9):2143–58. https://doi.org/10.1002/nme.116.

[55] Svanberg K. The method of moving asymptotes—a new method for structural optimization. : Int J Numer Methods Eng 1987;24(Nr. 2):359–73. https://doi.org/10.1002/nme.1620240207.